Exchange and anisotropy effects on spin waves in epitaxial Co films

M. Grimsditch and Eric E. Fullerton
Materials Science Division, Argonne National Laboratory, Argonne, Illinois 60439

R. L. Stamps
Department of Physics and Lima Campus, Ohio State University, Columbus, Ohio 43210

(Received 20 February 1997)

Using Brillouin scattering we have investigated the effect of large in-plane anisotropy on magnetic excitations in *b* axis-oriented epitaxial 50-nm Co films. For in-plane fields along the easy axis the magnon frequencies increase monotonically with increasing field. For in-plane fields along the hard axis, nonmonotonic behavior is observed in which the surface to bulk spin-wave character of one magnon mode changes as a function of applied field. Although fits to the data based on a full theoretical treatment are consistent with parameters in the literature and with parameters extracted from the magnetization data, we show that uncertainties in crystal orientation (as small as 1°) can produce dramatic effects in the quantitative data interpretation. [S0163-1829(97)06529-6]

I. INTRODUCTION

It is now possible to fabricate high-quality epitaxial hcp-Co films with the easy magnetization axis (the *c* axis of the hcp structure) lying in-plane. These films provide a unique opportunity to study spin-wave excitations in a system with a large in-plane anisotropy which is comparable in magnitude to the demagnetizing and applied fields. Infinite-wavelength excitations observed by ferromagnetic resonance techniques,[1] and the very short-wavelength excitations dominated by exchange interaction, investigated by neutron scattering,[2] are well understood in Co. The intermediate-wavelength regime, where exchange, anisotropy, applied, and demagnetizing fields all contribute significantly to the frequency of the excitations, has not yet been fully investigated. In this wavelength regime, which can be investigated using Brillouin scattering,[3–6] effects of exchange and propagation direction, not important in ferromagnetic resonance, must also be included. A detailed investigation, using Brillouin scattering, of the effects of anisotropy on spin excitations in single-crystal Fe has been presented in Ref. 6; the anisotropy, however, played only a small role.

Recently there has been considerable interest in cobalt with special attention being paid to its metastable fcc and bcc polymorphs. In the fcc and bcc forms the anisotropies are relatively small; Brillouin-scattering investigations[7,8] of these forms show the expected behavior similar to that found for Fe.[6] We are aware of only two investigations of hcp Co in the intermediate-wavelength regime probed by Brillouin scattering.[8,9] The investigation of Ref. 9 utilized a Co film which was *a*-axis oriented but polycrystalline in the plane. The polycrystalline nature of the material, which allowed the data to be analyzed assuming no anisotropy, produced results consistent with known values of the magnetization and gyromagnetic ratio. They did find however that the exchange stiffness constant was not in agreement with previously accepted bulk values determined by neutron scattering.[2] In Ref. 8 a *c*-axis-oriented hcp Co film was investigated; it was found that the Brillouin data was consistent with known anisotropy and magnetization. The exchange constant was again found to be inconsistent with the neutron data and the *g* factor was considerably lower than expected for hcp Co.

The samples used in Refs. 8 and 9 did not allow the effects of orientation to be investigated, in Ref. 9 because it was polycrystalline and in Ref. 8 because the demagnetizing fields kept the magnetization in the basal plane. With our epitaxial *b*-axis-oriented films we are able to observe the effects of the large anisotropy by probing different propagation and field directions. In addition, the film thickness is such that some of the bulk ''exchange'' modes are close in frequency to the surface mode. We are thereby also able to observe interactions between bulk and surface modes as the propagation direction with respect to the magnetization changes.

In the next section we present experimental data and compare our results with theoretical calculations. In particular, the pronounced effects of the large in-plane anisotropy on the spin-wave frequencies and their field dependence in different geometries is examined. Next, a sensitive dependence of the spin-wave frequencies on crystal and field orientation is described in Sec. III. Finally, the data taken from magnetization and Brillouin-scattering experiments allow a determination of values for the magnetization, exchange stiffness, first- and second-order anisotropies, and *g* factor. These values are discussed in Sec. IV and compared with results from previous experiments. An apparent inconsistency in measurements of the Co exchange constant is discussed.

II. EXPERIMENTAL RESULTS AND COMPARISON TO THEORY

The Co films were grown by magnetron sputtering onto Cr(211)-buffered MgO(110) single-crystal substrates. The Cr buffer layers were deposited at 600 °C and provide a lattice-matched template for *b*-axis Co (1010) films which were grown at 300 °C. The Co films were then capped with a 1.5-nm Cr layer to prevent oxidation. In addition to the Brillouin light-scattering studies, magnetization measurements

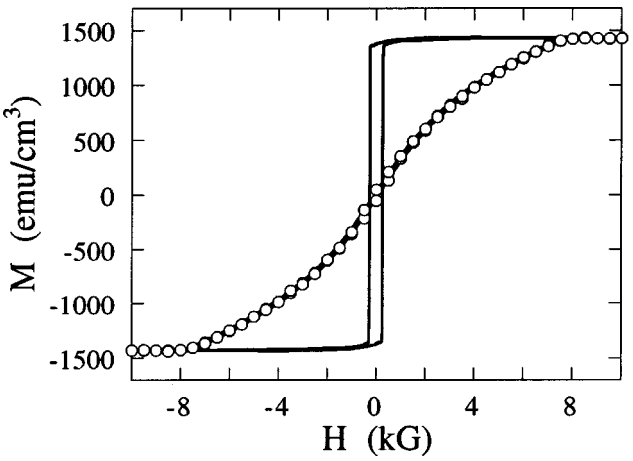

FIG. 1. Magnetization for applied fields in plane along the easy-axis (solid line) and hard-axis (open circles) directions. The line through the hard-axis data is a fit to Eq. (1) and the fitted values are given in Table I.

were made for in-plane fields H in the easy and hard directions. Figure 1 shows the measured magnetization loops for a 50-nm Co film with H applied along the hard (circles) and easy (full line) axes. The full line superimposed on the circles is a fit to the hard-axis data based on the energy expression:

$$E = K_1 \sin^2\theta + K_2 \sin^4\theta - MH\cos(\theta_H - \theta), \qquad (1)$$

where K_1 and K_2 are the first- and second-order anisotropies, θ is the angle between the magnetization M and the c axis, and θ_H is the angle between the applied field H and the c axis. The films are magnetized in-plane, so shape anisotropies serve to keep the magnetization in-plane but do not otherwise enter the energy in Eq. (1). The magnetization was obtained from the saturation value, and the anisotropies were obtained by fitting the hard-axis magnetization curve. The resulting values were in good agreement with those of bulk Co and are listed in Table I. Note that in order to reproduce the curvature of the magnetization in the hard direction it was necessary to include the higher-order anisotropy K_2. However, the value obtained for K_2 determined from fitting the hard-axis magnetization depends sensitively on the orientation of the sample and slight misalignments or mosaic spread of the c axis with respect to the applied field produces substantial changes in the fitted values. We shall return to this point in the last section.

Brillouin spectra were recorded in the quasibackscattering geometry with the incident beam at 60° from the surface normal and the scattered light collected along the surface normal. A $3+4$ pass Fabry-Perot interferometer was used to analyze the scattered 300 mW of 514.5 nm incident radiation. The scattered light was analyzed in crossed polarization to eliminate contributions to the spectra from surface phonons. All spectra were recorded at ambient temperature. The component of the wave vector parallel to the sample surface, determined by the scattering geometry, was 1.06×10^5 cm^{-1} and it was always perpendicular to the applied magnetic field. The sample could be rotated about its normal thereby allowing different propagation directions in the plane of the sample to be studied. The highest fields obtainable in our Brillouin experiments were just below 7 kG.

Figure 2(a) shows a spectrum obtained for a field of 1.5 kG along the easy axis. Following Ref. 10, the features in the spectrum are identified as a surface wave S or a bulk standing spin wave B_n, where the subscript n denotes the number of nodes across the film thickness. These latter modes correspond to guided ''bulklike'' magnons where the wave vector is quantized by the finite thickness of the sample. The surface mode S is identified by a large Stokes/anti-Stokes asymmetry in the scattering intensities.

The surface mode corresponds to the Damon-Eshbach mode on a semi-infinite ferromagnet. The Damon-Eshbach mode only propagates in directions near 90° as measured from the direction of the saturation magnetization. There is a critical propagation angle below which the Damon-Eschbach mode no longer exists. For the thin-film geometry considered here, this critical angle corresponds to a change from localized to bulk spin-wave behavior. This can be seen in the spectrum shown in Fig. 2(b) where a small field of 270 G is oriented along a hard direction. With this small field strength the magnetization is nearly aligned along the same direction that the measured spin waves propagate. This means that no surface mode exists and is evidenced by the nearly symmetrical scattering intensities, indicating no localization to the surface.

It is interesting to compare the behavior of the surface mode to the magnetostatic case considered in Ref. 15. The neglect of exchange in the magnetostatic limit is a standard approximation for thick films with a consequence that the surface mode merges into a bulk manifold at a critical value of the angle describing the propagation direction. Anisotropies can strongly influence the frequencies of the surface mode and bulk band limits, leading to several interesting

TABLE I. Magnetic parameters of Co determined by Brillouin light scattering (BLS), neutron scattering (NS), and magnetization (Mag).

Expt.	M_s (G)	g	K_1 (10^6 erg/cm^3)	K_2 (10^6 erg/cm^3)	D (meV Å^2)
Mag (this paper)	1430±100		3.4±0.4	1.1±0.4	
BLS (this paper)	1350±50	2.13±0.04	3.4±0.1	0.80±0.05	460±70
NS (Ref. 2)	1420				540±40
Mag (Ref. 17)	1450		3.0	1.3	
BLS (Ref. 8)		1.86±0.02	3.4±0.4		435±35
BLS (Ref. 9)	1330	2.16±0.02			340±75

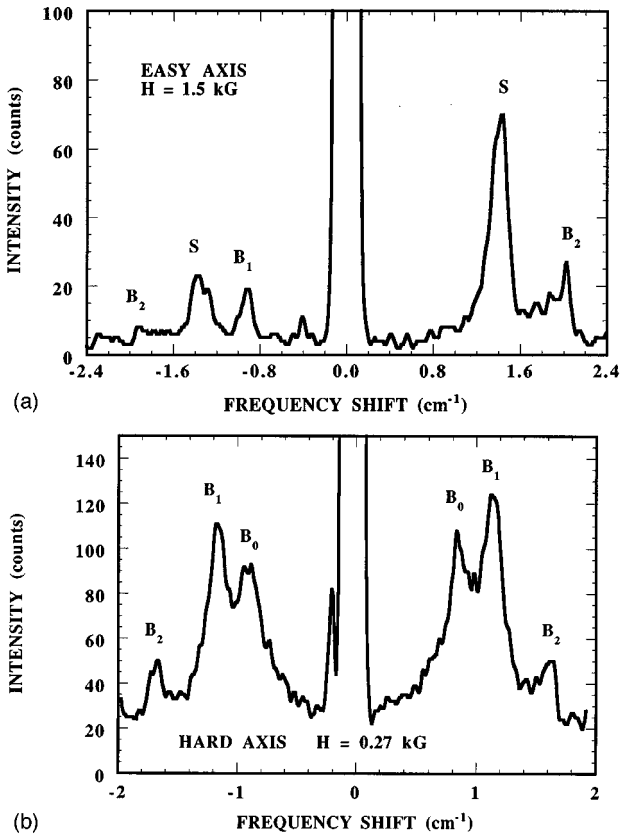

FIG. 2. Example Brillouin light-scattering spectra with the applied magnetic field along easy- and hard-axis directions. A 1.5 kG field is in the easy-axis direction in (a) and a small 270 G in-plane field is applied in a hard-axis direction in (b). The large Stokes/anti-Stokes asymmetry visible in (a) clearly identifies the surface mode. Note the absence of a surface mode in (b) due to the orientation of the saturation magnetization along the direction of propagation.

phenomena as discussed in Ref. 15. In the present thin-film case, there is no manifold of nearly degenerate bulk modes. Instead the surface mode can be uniquely identified as the lowest-order bulk spin wave. The effect of dipolar interactions is to shift the energy of this mode and localize it to one surface of the film. These effects are clearly evident in the frequency shifts and intensity ratios of the Brillouin spectra.

We now describe the data analysis. At 50 nm thick, the Co film supports bulk standing spin waves and a surface magnon with comparable frequencies. The frequencies of the modes therefore include contributions from exchange, Zeeman terms, anisotropies and ''demagnetizing'' fields, all of which must be properly described in the theory used for the data analysis. An appropriate theory is described in Refs. 11–13 and was modified for this problem to include uniaxial anisotropies and arbitrary (in-plane) orientations of the magnetization with respect to the applied field. We note that previous related calculations for spin waves with an emphasis on anisotropies presented in Refs. 14 and 15 did not include exchange contributions to the spin-wave frequencies. The theory discussed here is a generalization of these previous magnetostatic studies for thin-film geometries.

The mode frequency calculations are based on a long-wavelength semiclassical approximation that involves the following steps: (1) finding the equilibrium orientation of the magnetization determined by competition of the anisotropies and the applied field [Eq. (1)]; (2) writing the equations of motion describing torques acting on spins deviating slightly from the equilibrium orientation due to effective fields $\mathbf{H}_{\rm eff}$; (3) solving the linearized equations of motion, together with the appropriate electromagnetic and exchange boundary conditions, to obtain the frequencies of long-wavelength spin excitations.

Effective fields are found from $\mathbf{H}_{\rm eff}=-\nabla_{\mathbf{m}}F$ where F is an energy including exchange contributions due to spatial variations in the magnetization, the first- and second-order anisotropies, and the Zeeman energy. The time and spatially varying part of the magnetization is denoted by the vector $\mathbf{m}$. Effects due to shape demagnetizing fields enter via Maxwell's equations.

The fields are evaluated with the static magnetization along the equilibrium direction specified by θ which is in general different from θ_H except along special directions. Writing D as the usual exchange stiffness and q as the in-plane spin-wave wave vector, the torque equations are

$$dm_x/dt=\gamma[H\cos(\theta_H-\theta)+(2K_1/M)(1-2\sin^2\theta)+(4K_2/M)(\sin^2 2\theta-\sin^2\theta)-(D/\gamma)(q^2-d^2/dy^2)]m_y-\gamma M h_y, \quad (2)$$

$$dm_y/dt=-\gamma[H\cos(\theta_H-\theta)+(2K_1/M)\cos^2\theta+(K_2/M)\sin^2 2\theta-(D/\gamma)(q^2-d^2/dy^2)]m_x+\gamma M h_x. \quad (3)$$

Here m_x and m_y are the time and spatially varying components of the magnetization along directions perpendicular to the equilibrium (z) direction and y is along the surface normal. The gyromagnetic ratio is $\gamma=2\pi g\mu_B/h$. The anisotropy contributions to the effective fields are consistent with the energy as written in Eq. (1). Dynamic demagnetizing fields, which originate from Maxwell's equations, are represented by h_x and h_y. This means that in order to completely define the problem, in the magnetostatic limit the complete equations of motion must also include $\nabla\cdot(\mathbf{h}+4\pi\mathbf{m})=0$.

Figure 3 shows the frequency of the three modes observed in Fig. 2 as a function of field along the easy 3(a) and hard 3(b) axes. For H applied along the easy axis the frequency of all three modes increase monotonically with field; qualitatively this reflects the fact that at zero field the magnetization is already aligned along the easy axis so that the applied field does not compete with the anisotropy but simply contributes an additional torque. For H along the hard axis the frequencies of all three modes exhibit nonmonotonic behavior reflecting the ''reorientation'' of the sample magnetization as the field is applied. It is interesting to note that, in our scattering geometry where q is perpendicular to H, the B_0 mode (which as discussed above has no nodes across the film thickness) propagates parallel to M at zero field. At high fields B_0 no longer exists but is replaced by a surface mode that propagates perpendicular to M. The bulklike peaks B_2 and B_3 (whose wave vectors lie close to the surface normal) are always propagating perpendicular to M. The details of how the B_0 mode transforms to a surface mode are discussed below.

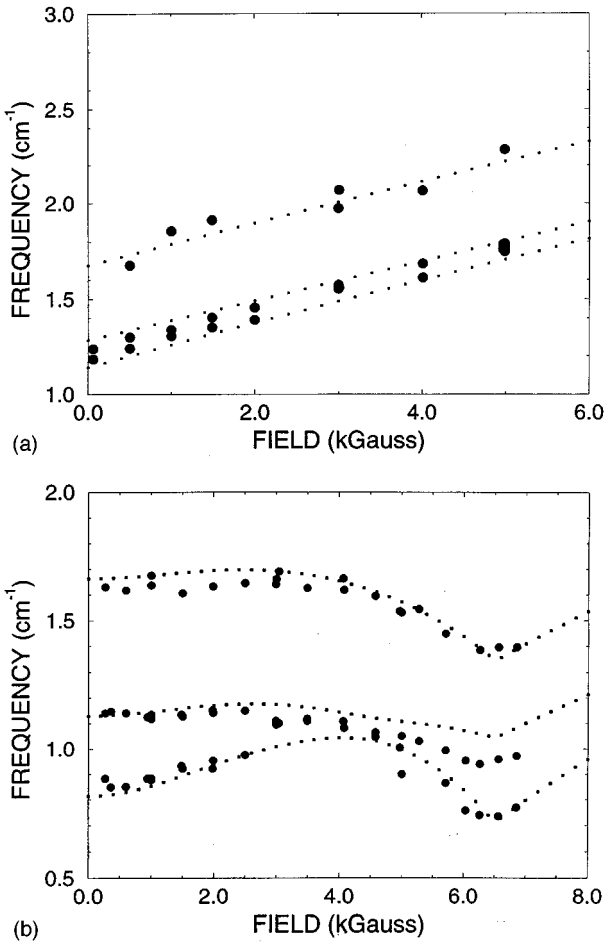

FIG. 3. Spin-wave frequencies as functions of applied field. Experimental results and theory are shown for the field aligned in the in-plane easy-axis (a) and hard-axis (b) directions. The large circles are data points taken from the spectra and the dotted lines are calculated using the theory described in the text. A mode crossing is evident in the hard-axis data (b). This is due to the increase in frequency of the lowest order bulk mode as the propagation direction changes. The mode becomes increasingly more surfacelike and crosses the B_1 bulk mode between 3 and 5 kG.

The small dots in Fig. 3 are the results of calculations where the individual parameters were determined as follows. The slope of the frequencies as a function of field along the easy direction yields g. The position of the frequency minimum (6.5 kG), which corresponds to the field at which the magnetization aligns with the field along the hard axis, is determined by K_1 and K_2. This region is very sensitive to the orientation of the crystal, and the consequences will be discussed in Sec. III. The difference in the ''hard'' and ''easy'' frequencies above saturation is also determined by K_1 and K_2. The overall frequency scale is determined mainly by $4\pi M$.

In addition to the anisotropies, frequency differences provide information about exchange. The 50-nm Co film thickness allows the measurement of two bulk spin-wave frequencies in addition to the surface-mode frequency. This provides a sensitive measure of the exchange since the difference in the frequencies of the two bulk modes is determined by D whereas the surface mode is insensitive to D. Values of the various parameters determined from the light-scattering analysis are listed in Table I together with estimated errors based on the range of allowable values that produce reasonable fits to the data.

The range of applied fields between zero and 5 kG from the hard-axis data is interesting because of the behavior of the surface mode. As the field is increased the magnetization rotates towards the direction of H and away from q. During this process the lowest frequency mode transforms into the surface mode. Localization of the long-wavelength spin wave to the surface is due to magnetostatic energies, and these also increase the frequency of the mode. In this case, the increase in frequency leads to a hybridization between the surfacelike mode and the lowest-frequency bulk mode (B_1).

Expected details of the mode ''crossing'' with H applied along the hard axis are displayed in Fig. 4. Calculated spectra are shown in (a) and were calculated along the lines of the theory given in Ref. 16 using the parameters given above and a small damping term. The calculated behavior reproduces the main features observed in the actual data: at low fields the Stokes/anti-Stokes asymmetries indicate that all modes are bulklike whereas at fields above 3 kG a clearly identifiable surface mode appears.

The scattering intensities can be understood in greater detail by studying the amplitudes of the fluctuating magnetization as a function of position in the film associated with the different spin-wave modes. The amplitudes in the plane of the film [the m_x of Eqs. (2) and (3)] for the two lowest frequency spin waves are shown as a function of depth in Fig. 4(b). The mode profile, determined by the thin-film geometry, allows the modes to be classified by the number of nodes n. At low fields it is the lowest-frequency mode which corresponds to $n=0$. This mode is localized to one surface when propagating near perpendicular with respect to the magnetization, as discussed before. Between 5 and 5.5 kG the node structure changes as the magnetization rotates and it is the second mode which has $n=0$ indicating that it has become the surfacelike magnetic excitation.

It is interesting to note that in order for the node structure to switch from one mode to another with increasing applied field, it is necessary for the amplitude at one surface to vanish for some applied field strength. A maximum in the Stokes/anti-Stokes ratio can then be expected. The spectra shown in Fig. 4(a) exemplify this behavior; at 5 kG the first (second) mode is notably absent on the Stokes (anti-Stokes) side of the spectrum. The intensities below 4 kG do not indicate any strongly localized surface mode, as expected. Between 5 and 6 kG, where the two lowest modes interact, large Stokes/anti-Stokes ratios appear. Above 6 kG the intensity ratios are consistent with the middle frequency mode being a strongly localized surface mode.

Experimental verification of the above conclusions is hampered by the closeness of the two modes which makes them experimentally unresolved. Furthermore it is not clear what the effects quadratic coupling between the magnetization and the light might play in the calculated spectra. The results presented above compare well with those presented in Ref. 4 where mode repulsion between the two lowest modes was also observed in the angular dependence for an iron film.

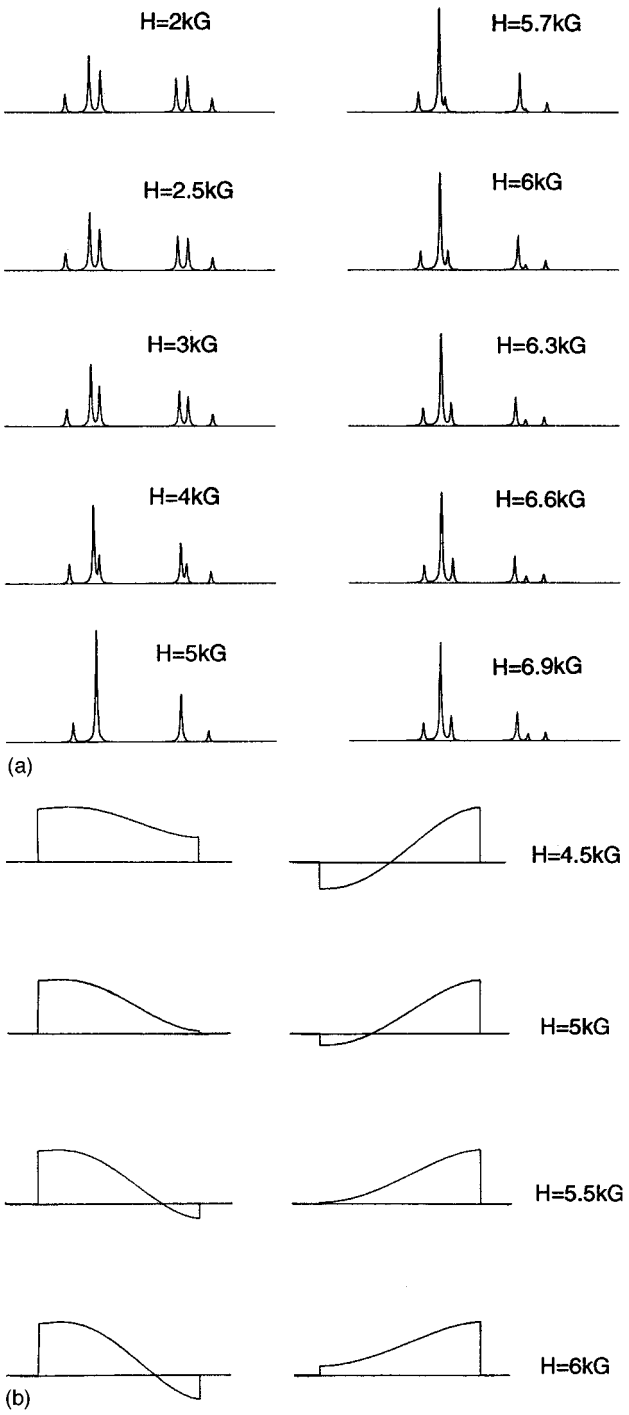

FIG. 4. Calculated scattering intensities and mode profiles. Calculated Stokes/anti-Stokes intensities are examined in (a) for the crossing region seen in Fig. 3(b). A maximum in the surface mode intensity ratio is predicted for applied fields where the two lowest frequency modes hybridize. This is due to the change between surface- and bulklike character of the two modes as illustrated in m_x profiles shown in (b). The m_x amplitudes shown in (b) are plotted as functions of position across the Co film. The horizontal lines are zero amplitude references.

III. EFFECTS OF MISALIGNMENT

As mentioned in the previous section the numerical values obtained for the magnetic parameters depend strongly on sample orientation. The equilibrium condition obtained from

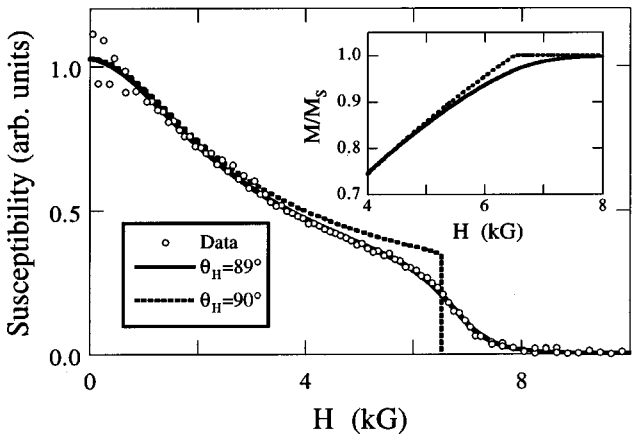

FIG. 5. Effects of a small misalignment on the hard-axis magnetization measurements. The calculated ac susceptibility and magnetization (inset) are shown as a function of applied field for $\theta_H = 89$ and 90°. The open circles are the ac-susceptibility data for a Co film. Even the small misalignment of 1° has a dramatic effect on the susceptibility near saturation.

Eq. (1) when H makes an angle θ_H with the easy axis is

$$dE/d\theta = 0 = 2K_1 \sin(\theta)\cos(\theta) + 4K_2 \sin^3(\theta)\cos(\theta) - MH\ \sin(\theta - \theta_H). \quad (4)$$

The measured magnetization is given by $M\ \cos(\theta - \theta_H)$. It is clear that for $\theta_H = 90°$ $[\sin(\theta - \theta_H) = \cos(\theta)]$ Eq. (4) can be simplified by dividing by $\cos(\theta)$ and the solution requires solving a cubic equation in $\sin(\theta)$. However, since this solution requires dividing by $\cos(\theta)$ it is no longer strictly valid above saturation when $\theta = 90°$. The solution to Eq. (4) for a general θ_H requires numerical techniques. The inset of Fig. 5 shows the calculated magnetization for $\theta_H = 90°$ and 89° near saturation. For $\theta_H = 90°$, there is a well defined saturation field H_S given by $(2K_1 + 4K_2)/M$. However, if the field is slightly misaligned from the hard axis, the magnetization approaches saturation asymptotically. This difference near saturation is clearly seen in the ac susceptibility shown in Fig. 5. For $\theta_H = 90°$ there is a discontinuity in the susceptibility at H_S. For $\theta_H = 89°$ the discontinuity is rounded and in close agreement with the experimental results for a Co film. Although this rounding at saturation is consistent with misalignment of the film, the present results cannot rule out that other effects, e.g., an in-plane mosaic spread of Co crystallites, may also contribute to the rounding. It is, however, clear from Fig. 5 that anisotropy parameters (especially K_2) extracted from magnetization loops will be sensitive to alignment even in the absence of mosaic spread.

A comparison of the magnon's calculated field dependence when H is applied at 90° and 89° is shown in Fig. 6. Here also it is clear that the frequency minima are dramatically affected by slight sample misorientation. The position of the minimum is also slightly displaced to higher fields. It is interesting to note that the sharpness of the minimum indicates the accuracy of the alignment: the dip is much more pronounced with good alignment. It is important to remember however that the magnon frequencies at low fields are also sensitive to the anisotropies. K_2 is especially important in determining the low-field frequencies of the hard-axis data, so that the light-scattering measurements provide valuable additional data not contained in pure magnetization measurements.

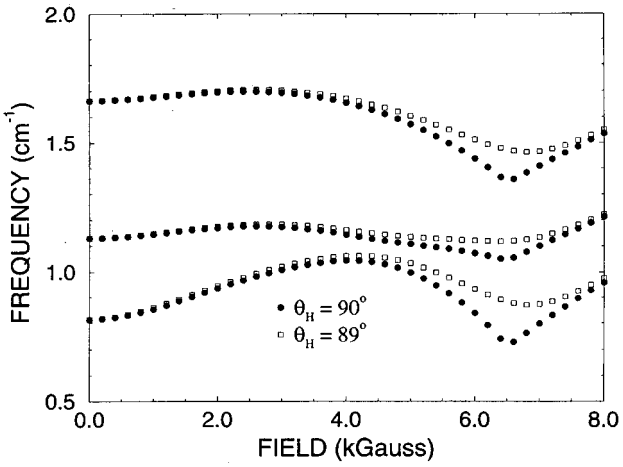

FIG. 6. Effects of a small misalignment on the spin-wave frequencies. Calculated spin-wave frequencies are shown as a function of applied field for $\theta_H = 89$ and 90°. The dark squares are for perfect alignment along the hard axis ($\theta_H = 90°$) and the open circles are for a 1° misalignment ($\theta_H = 89°$). The effect of misalignment is to shift the position of the frequency dip and reduce its sharpness.

The main conclusion is that the accurate determination of the anisotropies is largely limited by alignment. The limit currently achievable in our laboratory corresponds to an uncertainty of approximately ± 50 G for the values of the effective anisotropy field, as estimated by the uncertainty in the position of the minimum described above. This uncertainty is less consequential for the determination of other parameters M, g, and D, since these are primarily measured from aspects of the data that are not strongly dependent on alignment, as discussed in Sec. III. The error in D originates mainly from the uncertainty ($\approx 5\%$) in the film thickness.

IV. DISCUSSION AND CONCLUSIONS

The magnetic parameters determined with Brillouin light scattering in this study are summarized in Table I. Values obtained in the present study using magnetization measurements and literature values for bulk Co are also given. Except for one determination[8] all values of g are within the quoted uncertainties. It can be seen that our experimental values obtained by magnetization measurements and Brillouin light scattering are consistent. The small differences between the anisotropies we measured and those typical of bulk Co are most likely due to subtle changes induced by growth strains or other thin film effects.

More interesting are the lower values for D obtained in our and at least two other Brillouin works[8,9] compared to a value of 500–580 meV Å^2 obtained from neutron-scattering and magnetization measurements on bulk Co.[2,17] This discrepancy was in fact first noticed by Vernon *et al.*, in an earlier Brillouin light-scattering study of Co films with the suggestion that the average D measured in light scattering might be reduced in polycrystalline samples.[9] A more likely explanation for the discrepancy, recently brought to our attention by Cochran,[18] is based on pinning effects. Pinning modifies the location of the surface antinodes of the standing spin waves thereby changing their effective wavelength. Since the Brillouin frequencies depend on Dq^2 this translates into a decrease in the value extracted for D. The very limited available information on pinning precludes, at present, refinements of the calculations to include pinning effects in a reliable manner.

In conclusion, we have measured anisotropies, magnetization, and exchange stiffness constants for a uniaxial Co film grown with an in-plane c axis. Results for the anisotropies found from Brillouin light-scattering data were consistent with those determined by magnetization measurements. The exchange stiffness was found to agree with previous light-scattering results on Co films, but most Brillouin results disagree with earlier neutron-scattering measurements on bulk Co. Finally, we have also studied a hybridization between spin-wave modes driven by the long-range dipolar interaction. As a result, a change from bulk- to surfacelike character was observed as a function of applied field that strongly affected Stokes/anti-Stokes ratios. The experimental observations were consistent with theoretical calculations for the light-scattering intensities.

ACKNOWLEDGMENT

The work at ANL was supported by the U.S. Department of Energy, Basic Energy Sciences-Materials Sciences, under Contract No. W-31-109-ENG-38.

[1] M. B. Stearns, J. Appl. Phys. **53**, 2436 (1982).
[2] G. Shirane, V. J. Minkiewicz, and R. Nathans, J. Appl. Phys. **39**, 383 (1968).
[3] J. Sandercock, in *Light Scattering in Solids III*, edited by M. Cardona and G. Guntherodt (Springer, Berlin, 1982), p. 173.
[4] R. E. Camley and M. Grimsditch, Phys. Rev. B **22**, 5420 (1980).
[5] P. Grunberg, C. M. Mayr, W. Vach, and M. Grimsditch, J. Magn. Magn. Mater. **28**, 319 (1982).
[6] G. Rupp, W. Wettling, R. S. Smith, and W. Jantz, J. Magn. Magn. Mater. **45**, 404 (1984).
[7] P. Kramas, F. Lauks, R. L. Stamps, B. Hillebrands, and G. Guntherodt, Phys. Rev. Lett. **69**, 3674 (1992).
[8] X. Liu, M. M. Steiner, R. Sooryakumar, G. A. Prinz, R. F. C. Farrow, and G. Harp, Phys. Rev. B **53**, 12 166 (1996).
[9] S. P. Vernon, S. M. Lindsay, and M. B. Stearns, Phys. Rev. B **8**, 4439 (1984).
[10] M. Grimsditch, A. Malozemoff, and A. Brunsch, Phys. Rev. Lett. **43**, 711 (1979).
[11] R. E. Camley and D. L. Mills, Phys. Rev. B **18**, 4821 (1978).
[12] R. L. Stamps and B. Hillebrands, Phys. Rev. B **43**, 3532 (1991).
[13] S. Subramanian, X. Liu, R. L. Stamps, R. Sooryakumar, and G. A. Prinz, Phys. Rev. B **52**, 10 194 (1995).
[14] B. Schneider, Phys. Status Solidi B **51**, 325 (1972).
[15] M. J. Hurben and C. E. Patton, J. Magn. Magn. Mater. **162**, 39 (1996).
[16] J. R. Dutcher and J. F. Cochran, J. Magn. Magn. Mater. **72**, 307 (1988).
[17] R. Pauthenet, J. Appl. Phys. **53**, 8187 (1982).
[18] J. Cochran (private communication).